Technische Mechanik, Band 21, Heft 1, (2001), 1-12
Manuskripteingang: 23. Juni 2000

Local Buckling of Composite Laminated Cylindrical Shells with Oblique Edges under External Pressure: Asymptotic and Finite Element Simulations

G. Mikhasev, F. Seeger, U. Gabbert

The problem of local buckling of a thin composite laminated cylindrical shell under external pressure is studied. Each layer of the shell is assumed to be isotropic. The special case of the shell being non-circular and/or having no plane edges is considered here. Presupposing that buckling takes place in the neighborhood of some so-called "weakest" generator, the asymptotic Tovstik's method is applied finding the critical pressure and the eigenmodes. As an example, buckling of a three-layered circular thin cylinder with a sloped edge is investigated. Besides the asymptotic approach the finite element simulation is applied to facilitate the estimation of the range to which the results obtained can be applied.

1 Introduction

Thin composite laminated shells are used in many engineering structures, such as airborne/spaceborne vehicles, ships or underwater objects, etc. Buckling under external pressure of thin laminated cylinders or panel elements which are parts of these structures, is a subject of great practical interest (also refer to the list of papers in the books of Bolotin and Novichkov, 1980; and Grigoliuk and Kulikov, 1988). Most of the papers published are based on the assumption that cylindrical shells have constant geometrical parameters. In this case an exact solution of the problem of shell buckling can be found: the only difficulty is to choose a model (basic hypothesis) and a corresponding system of differential equations. Major problems, which have been rarely studied, occur when a cylindrical shell has a variable radius of curvature and/or a generatrix length, which make exact analytical methods impossible. Here, approximate, asymptotic, or numerical approaches can be more efficient.

A significant contribution to the development of asymptotic methods facilitating the analysis of buckling of isotropic one-layered cylindrical and conical shells with variable geometrical parameters has been made by Tovstik (1983). He proposed the approach for the cases when buckling occurs locally on the shell surface. According to this method the approximate solutions of the governing equations are constructed in the form of functions oscillating and quickly decreasing far from some generatrix named "weakest". Later, this method was applied to study buckling of isotropic non-circular conical shells with slanted edges under non-constant external pressure (Mikhasev and Tovstik, 1990). The underlying concepts of the new method as well as a great number of solved problems can be found in Tovstik's book (1995).

The present paper mainly aims to apply Tovstik's method (1995) to investigate buckling of a thin laminated non-circular cylindrical shell with slanted edges subjected to normal external pressure. The specific aim defined herein is to study the same problem utilizing the COSAR system (COSAR, 1990; Gabbert et al., 1990) based on the finite element simulation, and to compare the results of different approaches.

2 Setting a Problem

A thin cylindrical shell is considered consisting of N isotropic layers characterized by thickness h_k, the Young's modulus E_k and the Poisson's ratio ν_k, $k = 1, ..., N$. The original surface is assumed to be the middle surface of any fixed layer (see Figure 1).

For the orthogonal co-ordinate system (α_1, α_2, z) of the original surface assumptions are made as shown in Figure 1. The shell is non-circular (i.e. the radius of curvature $R_2(\alpha_2)$ is a function) and non-closed in the direction of the co-ordinate α_2 (i.e., a general cylindrical panel); its edges are not supposed to be plane curves: $L_1(\alpha_2) \le \alpha_1 \le L_2(\alpha_2)$. On the shell edges $\alpha_1 = L_j(\alpha_2)$ we consider one of two variants of boundary conditions (or their combination), i.e. the joint support conditions or the rigid clamp ones. Investigations focus on that case when the normal pressure Q_n is applied to the shell.

2.1 Basic Hypothesis

Presently the laminated shell theory has been developed into two basic directions. In the most general terms the theory of multilayer shells has been developed by Grigoliuk and Chulkov (1965), Hsu and Wang (1970),

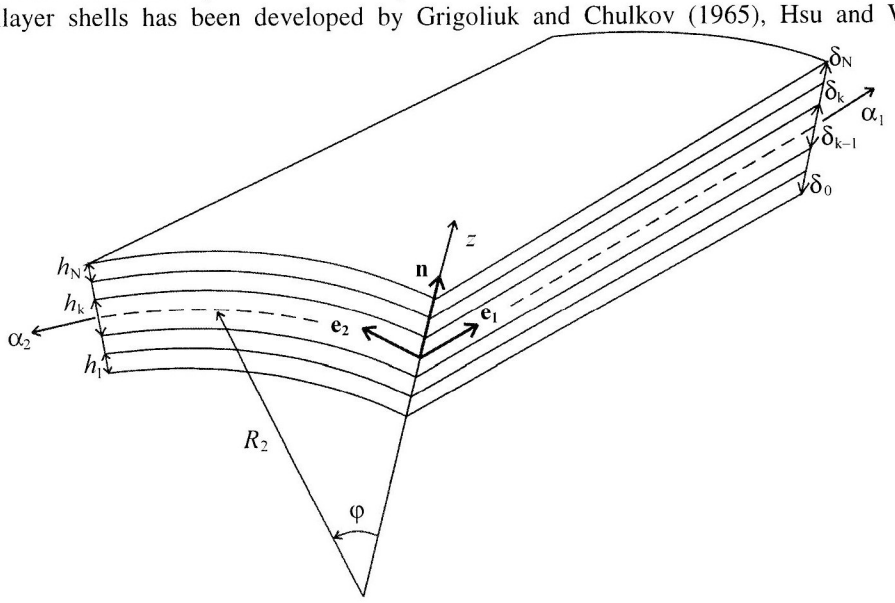

Figure 1. Laminated Cylindrical Shell and Co-ordinate System

Gotteland (1975), Chepiga (1976), Bolotin and Novichkov (1980). Their papers proceed from an order of shell equations depending on the number of layers of a shell.

The second approach to the laminated shell theory is based on an unique kinematics hypothesis (Grigoliuk and Kulikov, 1988). Although this approach is more common than the first one, it leads to a system of partial differential equations which does not depend on the number of layers. In some cases - in particular in cases where problems of buckling or vibrations of a laminated shell occur with only minor sizes of deflections or wave length - this system may be reduced to the system of two equations being analogous to Karman's equations. This simplified approach is utilized in the sections below.

To formulate the basic principle of the laminated shell theory used herein, it is necessary to introduce the additional notations. Let δ_k be the distance between the original surface and the upper bound of the k^{th} layer, $\tilde{u}_i$ and $\tilde{w}$ the tangential and normal displacements, respectively, of the original surface points, $\tilde{u}_i^{(k)}$ the tangential displacements of points of the k^{th} layer, σ_{i3} the transverse shear stresses, $\Theta_i^{(1)}$ the angles of rotation of the normal **n** around the vectors $\mathbf{e}_i$ (see Figure 1).

The following hypotheses (Grigoliuk and Kulikov, 1988) are assumed here:

1) The distribution law of the transverse tangent stresses across the thickness of the k^{th} layer is assumed to be of the form:

$$\sigma_{i3} = f_0(z)\,\mu_i^{(0)}(\alpha_1,\alpha_2) + f_k(z)\,\mu_i^{(k)}(\alpha_1,\alpha_2) \tag{1}$$

where $f_0(z), f_k(z)$ are continuous functions so that

$$f_0(\delta_0) = f_0(\delta_N) = 0 \qquad f_k(\delta_{k-1}) = f_k(\delta_k) = 0 \qquad f_k(z) = 0 \text{ at } z \notin [\delta_{k-1}, \delta_k] \tag{2}$$

2) Normal stresses acting on the area elements being parallel to the original one are negligible with respect to other components of the stress tensor.

3) The deflection $\tilde{w}$ is not a function of the co-ordinate z.

4) The tangential displacements are distributed across the thickness of the layer packet according to the generalized kinematic hypothesis of Timoshenko:

$$\tilde{u}_i^{(k)}(\alpha_1,\alpha_2,z)=\tilde{u}_i(\alpha_1,\alpha_2)+z\Theta_i^{(1)}(\alpha_1,\alpha_2)+g(z)\Theta_i^{(2)}(\alpha_1,\alpha_2) \tag{3}$$

where $g(z)=\int_0^z f_0(x)dx$. The functions $\mu_i^{(0)},\mu_i^{(k)},\Theta_i^{(2)}$ can be found in the book of Grigoliuk and Kulikov, (1988). It should be noted here that $\mu_i^{(0)},\mu_i^{(k)}$ are depend on the element of the matrix characterizing the transverse shifted pliability of the k^{th} layer. Hypothesis (3) permits the description of the non-linear dependence of the tangential displacements on the z co-ordinate; at $g\equiv 0$ it turns into Timoshenko's hypothesis.

2.2 Governing Equations

Based on the assumptions of the hypotheses 1 to 4 Grigoliuk and Kulikov (1988) derived a system of twelve non-linear equations describing the equilibrium of laminated anisotropic shells. We must assume here that buckling of the shell is accompanied by the formation of a large number of small dents. Proceeding from this assumption the foregoing system may be reduced to the following system (Grigoliuk and Kulikov, 1988):

$$\begin{aligned}\Delta^2\tilde{F}&=\frac{Eh}{R_2(\alpha_2)}\frac{\partial^2}{\partial\alpha_1^2}\left(1-\frac{h^2}{b}\Delta\right)\tilde{\chi}\\ D\left(1-\frac{\theta h^2}{b}\Delta\right)\Delta^2\tilde{\chi}&+\frac{1}{R_2(\alpha_2)}\frac{\partial^2\tilde{F}}{\partial\alpha_1^2}-T_2\frac{\partial^2}{\partial\alpha_2^2}\left(1-\frac{h^2}{b}\Delta\right)\tilde{\chi}=0\end{aligned} \tag{4}$$

where

$$h=\sum_{k=1}^{N}h_k\qquad \nu=\sum_{k=1}^{N}\frac{E_kh_k\nu_k}{1-\nu_k^2}\left(\sum_{k=1}^{N}\frac{E_kh_k}{1-\nu_k^2}\right)^{-1}\qquad E=\frac{1-\nu^2}{h}\sum_{k=1}^{N}\frac{E_kh_k}{1-\nu_k^2}\qquad D=\frac{Eh^3\eta_3}{12(1-\nu^2)}\qquad \tilde{w}=\left(1-\frac{h^2}{b}\Delta\right)\tilde{\chi}$$

Here Δ is the Laplace operator in the curvilinear co-ordinate system (α_1,α_2), $\tilde{F},\tilde{\chi}$ are the stress and displacement functions, respectively, h is the thickness, E, ν, D are the averaged Young's modulus, Poisson's ratio, and stiffness, respectively, $T_2=Q_n/R$ is the hoop stress due to the external normal pressure Q_n, R is the characteristic size of the shell which is defined below (see equation (25)); the parameters θ, b, η_3 take into account the averaged effects of shear in the shell and depend on the geometrical and physical properties of the layers:

$$\theta=1-\frac{\eta_2^2}{\eta_1\eta_3}\qquad b=\frac{12(1-\nu^2)q_{44}}{Eh\eta_1}\qquad \gamma_k=\frac{E_kh_k}{1-\nu_k^2}\left(\sum_{k=1}^{N}\frac{E_kh_k}{1-\nu_k^2}\right)^{-1} \tag{5}$$

$$\eta_1=\sum_{k=1}^{N}\varsigma_k^{-1}\pi_{1k}\gamma_k-3c_{12}^2\qquad \eta_2=\sum_{k=1}^{N}\varsigma_k^{-1}\pi_{2k}\gamma_k-3c_{13}c_{12}\qquad \eta_3=4\sum_{k=1}^{N}\left(\varsigma_k^2+3\zeta_{k-1}\varsigma_k\right)\gamma_k-3c_{13}^2$$

$$c_{12}=\sum_{k=1}^{N}\varsigma_k^{-1}\pi_{3k}\gamma_k\qquad c_{13}=\sum_{k=1}^{N}\left(\zeta_{k-1}+\zeta_k\right)\gamma_k\qquad G_k=\frac{E_k}{2(1+\nu_k)}$$

$$q_{44}=\frac{\left[\sum_{k=1}^{N}\left(\lambda_k-\frac{\lambda_{k0}^2}{\lambda_{kk}}\right)\right]^2}{\sum_{k=1}^{N}\left(\lambda_k-\frac{\lambda_{k0}^2}{\lambda_{kk}}\right)G_k^{-1}}+\sum_{k=1}^{N}\frac{\lambda_{k0}^2}{\lambda_{kk}}G_k\qquad \lambda_k=\int_{\delta_{k-1}}^{\delta_k}f_0^2(z)dz\qquad \lambda_{kn}=\int_{\delta_{k-1}}^{\delta_k}f_k(z)f_n(z)dz$$

$$\frac{1}{12}h^3\pi_{1k}=\int_{\delta_{k-1}}^{\delta_k}g^2(z)dz\qquad \frac{1}{12}h^3\pi_{2k}=\int_{\delta_{k-1}}^{\delta_k}zg(z)dz\qquad \frac{1}{2}h^2\pi_{3k}=\int_{\delta_{k-1}}^{\delta_k}g(z)dz$$

$$h\varsigma_k = h_k \qquad h\zeta_n = \delta_n$$

where the functions characterizing the distribution principle of the transverse shear stresses across the thickness are assumed as follows (Grigoliuk and Kulikov, 1988):

$$f_0(z) = \frac{1}{h^2}(z-\delta_0)(\delta_N - z) \qquad \text{at} \qquad z \in [\delta_0,\ \delta_N]$$

$$f_k(z) = \frac{1}{h_k^2}(z-\delta_{k-1})(\delta_k - z) \qquad \text{at} \qquad z \in [\delta_{k-1},\ \delta_k]$$

In equations (4) the shear influence is taken into account by the terms $h^2 b^{-1}\Delta\tilde{\chi}$, $\theta h^2 b^{-1}\Delta\tilde{\chi}$. If these terms equal zero, equations (4) degenerate into the well-known v. Kármán equations for elastic homogeneous shells.

3 Asymptotic Approach

Let the shell be sufficiently thin to facilitate applications of asymptotic methods. A small parameter ε is defined by

$$\varepsilon = \left\{h^2\eta_3 \Big/ \left[12\left(1-\nu^2\right)R^2\right]\right\}^{1/8}$$

Some further parameters are introduced by

$$\alpha_1 = Rs \qquad \alpha_2 = R\varphi \qquad R_2 = R/\rho(\varphi) \qquad T_2 = -\varepsilon^6 Eh\Lambda$$
$$\tilde{\chi} = R\chi \qquad \tilde{w} = Rw \qquad \tilde{F} = \varepsilon^4 EhR^2 F \qquad L_j = Rs_j(\varphi) \tag{6}$$

where the non-dimensional curvature $\rho(\varphi)$ is a two times differentiable function of φ (see Figure 1).
It is assumed that the shear parameters $K = \pi^2 h^2 \Big/ \left(bR^2\right)$ and θ are small:

$$K/\pi^2 = \varepsilon^2\kappa \qquad K\theta/\pi^2 = \varepsilon^3\tau \qquad \kappa, \tau \sim 1 \ \text{ at } \ \varepsilon \to 0 \tag{7}$$

These assumptions hold for a thin shell and those materials which are considered below as the components of the layer packet. Taking into account the relationships under (6) and (7), the equations (4) may be rewritten in the dimensionless form:

$$\varepsilon^4(1-\varepsilon^3\tau\Delta)\Delta^2\chi + \rho(\varphi)\frac{\partial^2 F}{\partial s^2} + \varepsilon^2\Lambda\frac{\partial^2}{\partial\varphi^2}(1-\varepsilon^2\kappa\Delta)\chi = 0$$

$$\varepsilon^4\Delta^2 F - \rho(\varphi)\frac{\partial^2}{\partial s^2}(1-\varepsilon^2\kappa\Delta)\chi = 0 \tag{8}$$

Let the shell edges $s = s_j(\varphi)$ be simply supported or clamped. A combination of these conditions may be also considered. The general order of the system (4) equals ten; therefore it is necessary to satisfy five boundary conditions on each edge. For example, for the simply supported cylinder these conditions may be written in terms of F and χ (Grigoliuk and Kulikov, 1988):

$$F = \Delta F = \chi = \Delta\chi = \Delta\Delta\chi = 0 \qquad \text{at} \qquad s = s_1(\varphi),\ s = s_2(\varphi) \tag{9}$$

The stress state of the shell comprises the basic stress state and the so-called edge-effect integrals, which are the solutions of the simplified equations describing the shell behavior near its edges (Gold'enveizer, 1961; Tovstik, 1995). Only two basic conditions have to be satisfied to fulfil the stress conditions on each edge. Apart from the terms of order ε^2 these conditions have the form (Tovstik, 1995) of

$$F = \chi = 0 \quad \text{and} \quad \chi = \partial\chi/\partial s = 0 \quad \text{at} \quad s = s_1(\varphi),\ s = s_2(\varphi) \tag{10}$$

for the joint support and rigid clamp conditions, respectively.
The problem is to find the minimum eigenvalue Λ for the boundaryvalue problem equations (8) to (10). Due to the variability of the curvature $\rho(\varphi)$ and the presence of the sloping edges $s_i(\varphi)$, it is assumed that the shell has the "weakest" generator $\varphi = \varphi_0$ (Tovstik, 1995) in the neighborhood where its buckling occurs. The functions $\rho(\varphi)$, $s_i(\varphi)$ are expanded into series in a vicinity of the line $\varphi = \varphi_0$:

$$\begin{gathered}\varphi - \varphi_0 = \varepsilon^{1/2}\xi \qquad \rho(\varphi) = \rho(\varphi_0) + \varepsilon^{1/2}\rho'(\varphi_0)\xi + \tfrac{1}{2}\varepsilon\rho''(\varphi_0)\xi^2 + \ldots \\ s_j(\varphi) = s_j(\varphi_0) + \varepsilon^{1/2}s_j'(\varphi_0)\xi + \tfrac{1}{2}\varepsilon s_j''(\varphi_0)\xi^2 + \ldots \qquad j=1,2\end{gathered} \tag{11}$$

In view of the conjectural localization of the eigenmodes, the solution of the boundaryvalue problem according to equations (8) to (10) is assumed to be of the form

$$\chi = \sum_{j=0}^{\infty} \varepsilon^{j/2}\chi_j(\xi, s)\exp\left\{\mathrm{i}\left(\varepsilon^{-1/2}q\,\xi + \tfrac{1}{2}a\,\xi^2\right)\right\} \qquad F = \sum_{j=0}^{\infty} \varepsilon^{j/2}F_j(\xi, s)\exp\left\{\mathrm{i}\left(\varepsilon^{-1/2}q\,\xi + \tfrac{1}{2}a\,\xi^2\right)\right\} \tag{12}$$

$$\Lambda = \Lambda_0 + \varepsilon\Lambda_1 + \varepsilon^2\Lambda_2 + \ldots \qquad \operatorname{Im} a > 0 \tag{13}$$

where $\chi_j(\xi, s)$, $F_j(\xi, s)$ are polynomials in ξ, q is the wave number, the symbol Im denotes the imaginary part, and the parameter a characterizes the rate of decay of the deflection amplitude when the distance from the weakest generator $\varphi = \varphi_0$ increases. The real and the imaginary parts of the functions (12), with taken into account the last inequality in equation (13), define the two eigenmodes localized near the line $\varphi = \varphi_0$.
Introducing the equations (10) to (13) into the equations (8) and eliminating the functions F_j, results in the following sequence of equations

$$\mathbf{H}_0\chi_0 = 0 \tag{14a}$$

$$\mathbf{H}_0\chi_1 + \mathbf{H}_1\chi_0 = 0 \tag{14b}$$

$$\mathbf{H}_0\chi_2 + \mathbf{H}_1\chi_1 + \mathbf{H}_2\chi_0 = 0, \text{ etc.} \tag{14c}$$

with

$$\mathbf{H}_0 z = \frac{\partial^4 z}{\partial s^4} + \frac{q^4\left[q^4 - \Lambda_0 q^2(1+\kappa q^2)\right]}{\rho^2(\varphi_0)(1+\kappa q^2)}z = 0 \tag{15}$$

$$\mathbf{H}_1 z = \left(a\frac{\partial \mathbf{H}_0}{\partial q} + \frac{\partial \mathbf{H}_0}{\partial \varphi_0}\right)\xi z - \mathrm{i}\frac{\partial \mathbf{H}_0}{\partial q}\frac{\partial z}{\partial \xi} \qquad \mathbf{H}_2 z = \frac{1}{2}\left(a^2\frac{\partial^2 \mathbf{H}_0}{\partial q^2} + 2a\frac{\partial^2 \mathbf{H}_0}{\partial q\,\partial \varphi_0} + \frac{\partial^2 \mathbf{H}_0}{\partial \varphi_0^2}\right)\xi^2 z -$$
$$-\mathrm{i}\left(a\frac{\partial^2 \mathbf{H}_0}{\partial q^2} + \frac{\partial^2 \mathbf{H}_0}{\partial q\,\partial \varphi_0}\right)\xi\frac{\partial z}{\partial \xi} - \frac{1}{2}\frac{\partial^2 \mathbf{H}_0}{\partial q^2}\left(\mathrm{i}\,z + \frac{\partial^2 z}{\partial \xi^2}\right) - \frac{\mathrm{i}}{2}\frac{\partial^2 \mathbf{H}_0}{\partial q\,\partial \varphi_0}z + \mathbf{H}_* z - \Lambda_1 q^2 z$$

where

$$\mathbf{H}_* = \frac{q^6 \tau}{\rho^2(\varphi_0)(1+\kappa q^2)} z$$

In case of simply supported edges, the equations (11) and (12) together with the boundary conditions (10) at $s = s_i(\varphi_0)$ result in the following sequence of boundary conditions for the functions $\chi_j(\xi, s)$:

$$\chi_0 = 0 \qquad \frac{\partial^2 \chi_0}{\partial s^2} = 0 \tag{16a}$$

$$\chi_1 + \xi s_j' \frac{\partial \chi_0}{\partial s} = 0 \qquad \frac{\partial^2 \chi_1}{\partial s^2} + \xi s_j' \frac{\partial^3 \chi_0}{\partial s^3} = 0 \tag{16b}$$

$$\begin{aligned} &\chi_2 + \xi s_j' \frac{\partial \chi_1}{\partial s} + \frac{\xi^2}{2}\left(s_j'^2 \frac{\partial^2 \chi_0}{\partial s^2} + s_j'' \frac{\partial \chi_0}{\partial s} \right) = 0 \\ &\frac{\partial^2 \chi_2}{\partial s^2} + \xi s_j' \frac{\partial^3 \chi_1}{\partial s^3} + \frac{\xi^2}{2}\left(s_j'^2 \frac{\partial^4 \chi_0}{\partial s^4} + s_j'' \frac{\partial^3 \chi_0}{\partial s^3} \right) - \frac{4 i s_j' \partial^3 \chi_0}{q \quad \partial s^3} = 0 \end{aligned} \tag{16c}$$

where the last condition (16c) is obtained from the second equation of (8). By analogy, the sequence of the boundary conditions for the clamped edges is derived:

$$\chi_0 = 0 \qquad \frac{\partial \chi_0}{\partial s} = 0 \tag{17a}$$

$$\chi_1 + \xi s_j' \frac{\partial \chi_0}{\partial s} = 0 \qquad \frac{\partial \chi_1}{\partial s} + \xi s_j' \frac{\partial^2 \chi_0}{\partial s^2} = 0 \tag{17b}$$

$$\begin{aligned} &\chi_2 + \xi s_j' \frac{\partial \chi_1}{\partial s} + \frac{\xi^2}{2}\left(s_j'^2 \frac{\partial^2 \chi_0}{\partial s^2} + s_j'' \frac{\partial \chi_0}{\partial s} \right) = 0 \\ &\frac{\partial \chi_2}{\partial s} + \xi s_j' \frac{\partial^2 \chi_1}{\partial s^2} + \frac{\xi^2}{2}\left(s_j'^2 \frac{\partial^3 \chi_0}{\partial s^3} + s_j'' \frac{\partial^2 \chi_0}{\partial s^2} \right) = 0 \end{aligned} \tag{17c}$$

3.1 Zeroth Order Approximation

In the zeroth order approximation the homogeneous differential equation holds true

$$\mathbf{H}_0 \chi_0 \equiv \frac{\partial^4 \chi_0}{\partial s^4} + \frac{q^4 \left[q^4 - \Lambda_0 q^2 (1+\kappa q^2) \right]}{\rho^2(\varphi_0)(1+\kappa q^2)} \chi_0 = 0 \tag{18}$$

with the homogeneous boundary conditions (16a) or (17a). This boundaryvalue problem has the solution

$$\chi_0(\xi, s) = P_0(\xi) \chi_0^\circ(\alpha x) \qquad \Lambda_0(q, \varphi_0) = \frac{\alpha^4 \rho^2(\varphi_0)}{q^6 l^4(\varphi_0)} + \frac{q^2}{1+\kappa q^2} \tag{19}$$

where $P_0(\xi)$ is an unknown polynomial in ξ, $l(\varphi_0) = s_2(\varphi_0) - s_1(\varphi_0)$, and α and $\chi_0^\circ(\alpha x)$ are the smallest positive eigenvalue and eigenfunction, respectively, of the equation $d^4z/dx^4 - \alpha^4 z = 0$. If both edges are simply supported the results are

$$\chi_0^\circ(\alpha x) = \sin(\alpha x) \qquad \alpha = \pi \qquad x = \left[s - s_1(\varphi_0)\right]/l(\varphi_0) \tag{20}$$

If the edge $s = s_2(\varphi_0)$ is clamped and the edge $s = s_1(\varphi_0)$ is simply supported the results are

$$\chi_0^\circ(\alpha x) = \frac{\sin(\alpha x)}{\sin\alpha} - \frac{\sinh(\alpha x)}{\sinh\alpha} \qquad \alpha = 3.9266 \qquad x = \left[s - s_1(\varphi_0)\right]/l(\varphi_0) \tag{21}$$

If both edges are clamped the results are

$$\chi_0^\circ(\alpha x) = \frac{\cos(\alpha x)}{\cos(\alpha/2)} - \frac{\cosh(\alpha x)}{\cosh(\alpha/2)} \qquad \alpha = 4.73 \qquad x = \left[s - s_1(\varphi_0)\right]/l(\varphi_0) - 1/2 \tag{22}$$

Minimizing the function $\Lambda_0(q, \varphi_0)$ over q, φ_0, we obtain

$$\Lambda_0^\circ = \Lambda_0(q_0, \varphi_0^\circ) = \frac{8}{3^{3/2}\alpha^2\kappa^3\Psi^\circ\vartheta^{\circ 3}} + \frac{3^{1/2}\alpha^2\kappa\Psi^\circ\vartheta^\circ}{2 + 3^{1/2}\alpha^2\kappa^2\Psi^\circ\vartheta^\circ} \qquad q_0^2 = \frac{3^{1/2}\kappa\alpha^2\Psi^\circ\vartheta^\circ}{2} \tag{23}$$

where

$$\vartheta^\circ = 1 + \sqrt{1 + \frac{4}{3^{1/2}\alpha^2\kappa^2\Psi^\circ}} \qquad \Psi(\varphi) = \frac{\rho(\varphi)}{l^2(\varphi)} \qquad \Psi^\circ = \Psi(\varphi_0^\circ)$$

The weakest generator $\varphi = \varphi_0^\circ$ is determined from the equation

$$\frac{d\Psi}{d\varphi} = 0 \tag{24}$$

It is assumed here that $\dfrac{d^2\Psi}{d\varphi^2} > 0$ at $\varphi = \varphi_0^\circ$. In particular, it may be seen from (24) that in a circular cylindrical shell the weakest generator is the longest one. Now, the characteristic size of the shell can be introduced as follows

$$R = R_2(\varphi_0^\circ) \tag{25}$$

3.2 First and Second Order Approximations

The first order approximation is characterized by the non-homogeneous equations (14b) with the non-homogeneous boundary conditions (16b) or (17b). The latter has a solution of the form (Tovstik, 1995)

$$\chi_1(\xi, s) = P_1(\xi)\chi_0^\circ + \xi P_0(a\chi_q + \chi_\varphi) - iP_0'\chi_q \tag{26}$$

where $P_1(\xi)$ is again an unknown polynomial in ξ, and the subscriptions q, φ denote differentiation with respect to q and φ, respectively. It should be noted that the existence condition of solution (26) is identical to the necessary condition of minimizing the function $\Lambda_0(q, \varphi_0)$.

In the second order approximation, we obtain again the non-homogeneous boundaryvalue problems of (14c), and (16c) or (14c) and (17c). The compatibility condition for this problem allows to find the parameters a, Λ_1 and the polynomial $P_0(\xi)$. Omitting details of all calculations (which can be found in Tovstik, 1995), we obtain

$$a = \mathrm{i}\sqrt{\frac{\Lambda_{\varphi\varphi}}{\Lambda_{qq}}} \qquad \Lambda_1 = \frac{1}{2}\sqrt{\Lambda_{\varphi\varphi}\Lambda_{qq}} + \frac{\tau q_0^4}{(1+\kappa q_0^2)} \qquad P_0 \equiv 1 \tag{27}$$

$$\Lambda_{qq} = \frac{42\,\alpha^4 \Psi^{\circ 2}}{q_0^8} + \frac{2(1-2\kappa q_0^2 - 3\kappa^2 q_0^4)}{(1+\kappa q_0^2)^4} \qquad \Lambda_{\varphi\varphi} = \frac{2\alpha^4}{q_0^6}\Psi^{\circ}\Psi''(\varphi_0^{\circ}) \tag{28}$$

A polynomial $P_1(\xi)$ is unknown in this approximation. To find it, it is necessary to consider the following two approximations. However, for developing the higher approximations the governing equations of (4) as well as the boundary conditions (10) should be specified (in particular, the edge-effect integral must be taken into account). Finally, we obtain the following approximate formula for the buckling pressure:

$$Q_n^* = \varepsilon^6 E h R\left[\Lambda_0 + \varepsilon\Lambda_1 + O\left(\varepsilon^2\right)\right] \tag{29}$$

where Λ_0, Λ_1 are defined by the equations (19) and (27), and the parameters E, h, R, ε are introduced according to equations (4) to (6). The symbol $O\left(\varepsilon^2\right)$ represents the quantities having the order ε^2, which have not been written out here.

The dimensionless normal deflection w and the displacement function χ are linked by the following correlation $w = (1-\varepsilon^2\kappa\Delta)\chi$. Taking into account equation (12) and separating the real and imaginary parts, the following two eigenmodes are obtained

$$\begin{aligned}
\tilde{w}_1 &= R\left[\chi_0^{\circ}(s) + O\left(\varepsilon^{1/2}\right)\right]\exp\left\{-\frac{1}{2}\varepsilon^{-1}\sqrt{\frac{\Lambda_{\varphi\varphi}}{\Lambda_{qq}}}\left(\varphi-\varphi_0^{\circ}\right)\right\}\cos\left[\varepsilon^{-1}q_0\left(\varphi-\varphi_0^{\circ}\right)+\phi\right] \\
\tilde{w}_2 &= R\left[\chi_0^{\circ}(s) + O\left(\varepsilon^{1/2}\right)\right]\exp\left\{-\frac{1}{2}\varepsilon^{-1}\sqrt{\frac{\Lambda_{\varphi\varphi}}{\Lambda_{qq}}}\left(\varphi-\varphi_0^{\circ}\right)\right\}\sin\left[\varepsilon^{-1}q_0\left(\varphi-\varphi_0^{\circ}\right)+\phi\right]
\end{aligned} \tag{30}$$

which correspond to the critical pressure in equation (29). Thus, the buckling pressure (29) is asymptotically a double root. It should be noticed that the method utilized here does not permit to define an initial phase ϕ.

4 Finite Element Simulation of Shell Buckling

For the finite element analysis of the buckling behaviour of shells the *SemiLoof* element family of the general purpose finite element package COSAR was used. The *SemiLoof* elements have been preferred due to their good overall accuracy in most shell applications and robustness compared with other possible finite shell elements. Originally, the *SemiLoof* element family was proposed by Irons (1976). In COSAR a curved six node triangualar and an eight node quadrilateral element with 24 and 32 degrees of freedom (*dof*), respectively, can be used. These *dof*s are the 3 displacements at each node, and additionally, the 2 tangential rotation at the 2 Gaussian integration points on each edge. The displacements and rotations are approximated by two families of shape functions, *Lagrangian* polynomials are used for the displacements and *Legendre* polynomials are employed for the rotations. The element has $C^{(0)}$ continuity along the edges and a pointwise $C^{(1)}$ continuity at the *Loof*-nodes (the 2 *Gaussian* integration points on the edges). The element fulfils the patch test. In order to simulate different material layers the classical laminate theory (CLT) is used. In buckling analysis a second order theory is used (classical stability problem) to calculate the critical eigenvalues from the eigenvalue problem

$$(\mathbf{K} - \lambda\mathbf{K}_\sigma)\mathbf{u} = \mathbf{0} \tag{31}$$

with the usual linear stiffness matrix $\mathbf{K}$, the geometric or initial stress matrix $\mathbf{K}_\sigma$, the eigenvalue λ and the eigenvector $\mathbf{u}$. In this stability problem a single parameter load is considered where the critical stress state σ_c (first critical buckling point) is calculated from an initial stress state $\hat{\boldsymbol{\sigma}}$

$$\boldsymbol{\sigma}_c = \lambda \hat{\boldsymbol{\sigma}} \tag{32}$$

caused by the initial load state. The initial stress state is calculated from a first linear solution of the cylindrical shell under the initial load state. In a second step the eigenvalue problem equation (31) is solved where the eigenvalue λ is the load parameter. The matrix $\mathbf{K}$ is assembled from the original linear stiffness matrices of the shell elements and the matrix $\mathbf{K}_\sigma$ is assembled from the following geometric element stiffness matrices (Zienkiewicz, 1977)

$$\mathbf{K}_\sigma^{(e)} = \int_V \mathbf{G}^T \hat{\boldsymbol{\sigma}} \mathbf{G} dV \tag{33}$$

where $\mathbf{G}$ contains the displacement gradient expressed by the shape functions and the initial element stress state $\hat{\boldsymbol{\sigma}}$ from the first calculation. The solution of the eigenvalue problem (31) results in the load factor λ, and the critical load level can be calculated by equation (32). For the analysis of the considered cylindrical structure a finite element mesh with a sufficient number of elements in longitudinal and circumferential direction has to be chosen to calculate the buckling load with sufficient accuracy. Especially if the buckling mode corresponds to a high wave number, a corresponding mesh density is required to ensure sufficient accuracy of the eigenvalues.

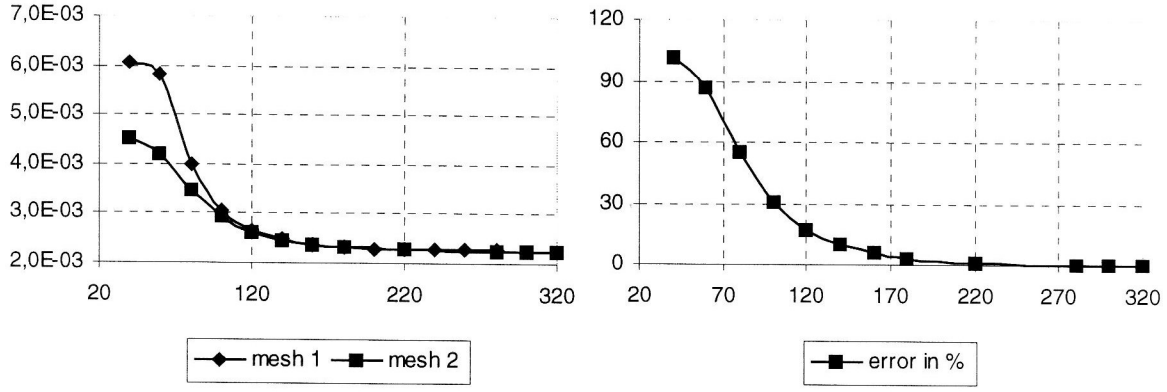

a) eigenvalue λ

b) error of the eigenvalue for mesh 2

Figure 2. Convergence of the Buckling Load in Dependence of the Number of Elements in Circumferential Direction, Mesh 1: 10 Elements and Mesh 2: 20 Elements in Longitudinal Direction.

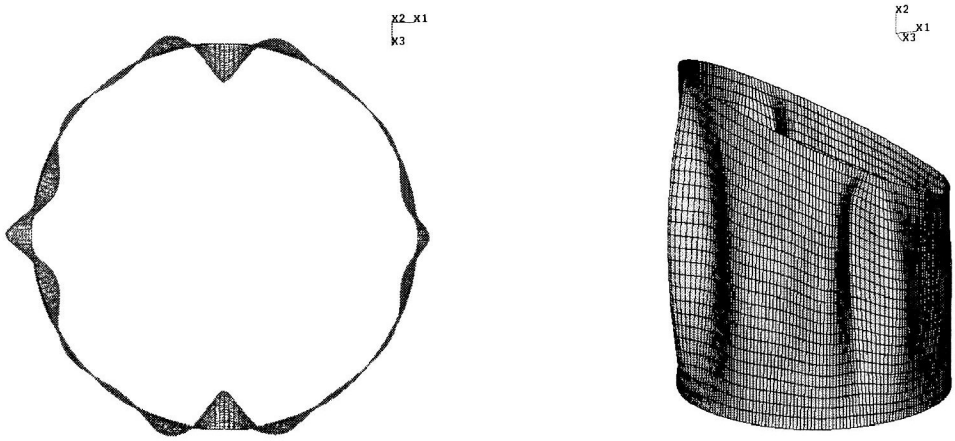

Figure 3. First Buckling Mode of the Cylinder with β=30°, h_2=0.0, Clamped - Simply Supported

The first tests revealed that the first buckling mode always corresponds to a higher wave number in circumferential direction, whereas in longitudinal direction only one wave occurs. Several test calculations where performed to study the convergence behaviour of the solution resulting in a high number of elements in circumferential direction and a lower number of elements in longitudinal direction (see Figure 2). The convergence test was performed to find the minimum number of elements providing an acceptable accuracy. The cylinder type with β=20°, clamped oblique and simply supported straight edges and h_2=0.002 mm was modeled to perform the convergence test (see Figure 5). With a number of 300 elements in circumferential direction the eigenvalue converges to the final value. The number of elements over the height does not influence the accuracy of the results. Figure 3 shows the first buckling mode of the cylinder with β = 30°, h_2=0.0 mm, clamped oblique edge and sim-

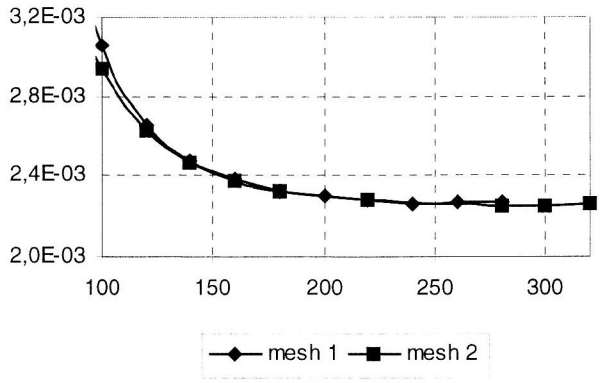

Figure 4. Convergence of the Buckling Load for the Range of 100 – 300 Elements in Circumferential Direction (see Figure 2)

ply supported straight edge. Figure 4 presents the development of the error in the buckling load as a function of the number of elements in circumferential direction.

5 Example: Asymptotic and Finite Element Simulations

As an example, the three-layered circular thin cylinder with sloped edge is considered (see Figure 5). Here

$$\rho = 1 \qquad s_1 = 0 \qquad s_2(\varphi) = l_0 + (\cos\varphi - 1)\tan\beta$$

where β is the inclination angle of the upper edge, $L = Rl_0 = 200$ mm is the maximum length of the shell, R = 80 mm is the shell radius. The first and third layers having the thickness $h_1 = h_3$ = 0.05mm are made of aluminum with the Young's modulus $E_1 = E_3$ = 70300 N/mm^2 and the Poisson's ratio $\nu_1 = \nu_3 = 0.345$, and the second one is an epoxy matrix with E_2=3450 N/mm^2, $\nu_2 = 0.3$. As can be seen, the longest generator $\varphi_0^\circ = 0$ is the "weakest" one, i.e. shell buckling occurs in the vicinity of the longest generator.

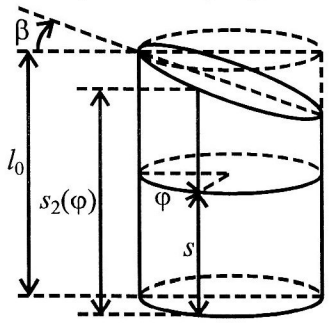

Figure 5 . Thin Circular Shell with the Oblique Edge

The dependence of the buckling pressure Q^*_n on the thickness h_2 and the angle β for two variants of boundary conditions and their combination are shown in Tables 1 to 3. It should be noted that the assumptions (7) introduced above hold true for all parameters taken into consideration.

h_2, mm	0	0,001	0,005	0,01	0,05	0,1	0,2
$\beta = 20^\circ$							
$10^5 Q_n^*$, N/mm^2 Asymptotic approach	233	238	260	289	573	1030	2250
$10^5 Q_n^*$, N/mm^2 Finite element simulation	230	235	256	284	561	1010	2196
$\beta = 30^\circ$							
$10^5 Q_n^*$, N/mm^2 Asymptotic approach	236	242	264	293	582	1050	2300
$10^5 Q_n^*$, N/mm^2 Finite element simulation	228	233	254	281	551	997	2178

Table 1. Dependence of the Buckling Pressure Q^*_n on h_2 and β when Both Edges are Clamped

h_2, mm	0	0,001	0,005	0,01	0,05	0,1	0,2
$\beta = 20^\circ$							
$10^5 Q_n^*$, N/mm^2 Asymptotic approach	194	199	217	241	478	864	1880
$10^5 Q_n^*$, N/mm^2 Finite element simulation	196	201	219	245	482	871	1904
$\beta = 30^\circ$							
$10^5 Q_n^*$, N/mm^2 Asymptotic approach	197	202	221	245	487	881	1920
$10^5 Q_n^*$, N/mm^2 Finite element simulation	197,1	201,5	219,8	244	477	868	1888

Table 2. Dependence of the Buckling Pressure Q^*_n on h_2 and β when the Oblique Edge is Clamped and the Straight Edge is Simply Supported

h_2, mm	0	0,001	0,005	0,01	0,05	0,1	0,2
$\beta = 20^\circ$							
$10^5 Q_n^*$, N/mm^2 Asymptotic approach	157	160	175	194	386	698	1520
$10^5 Q_n^*$, N/mm^2 Finite element simulation	162	165	181	201	398	725	1595
$\beta = 30^\circ$							
$10^5 Q_n^*$, N/mm^2 Asymptotic approach	160	163	178	198	394	713	1560
$10^5 Q_n^*$, N/mm^2 Finite element simulation	160	163,6	178,4	198,1	398	717	1593

Table 3. Dependence of the Buckling Pressure Q^*_n on h_2 and β when Both Edges are Simply Supported

It can be seen that increasing the angle β of inclination results in an increase of the critical pressure. An estimation of the influence of shear parameters κ, τ on the critical pressure indicates that this influence is insignificant. In some cases it hardly reaches 1% (for the shell with $\beta = 20^\circ$, $h_2 = 0.01$mm when both edges are simply supported). Calculations carried out by Grigoliuk and Kulikov (1988) revealed that this influence grows with a higher number of layers having essentially different physical properties. In our case the governing parameters are the averaged Young's modulus E, the Poisson's ratio ν, and the stiffness D.

We also performed a finite element simulation to estimate the range of application of the asymptotic approach (see Tables 1 to 3). The analysis of the calculations revealed that the divergence of the results obtained by the as-

ymptotic and numerical approaches increases with the thickness h_2 of the internal layer. This fact is attributable to a higher error rate of the asymptotic method when the shell thickness is increased.

Acknowledgement
This work was partly supported by the DAAD and the Byelorussian Education Ministry.

Literature

1. Bolotin, V. V., Novichkov Yu. N.: Mechanics of multilayer constructions, Mashinostroenie, Moskow, (1980), 376.
2. Chepiga, V. E.: On refined theory of laminated shells, Prikl. Mekh., Vol. 12, No. 11, (1976), 45-49.
3. COSAR: General purpose finite element package - User Manual (in German). FEMCOS GmbH Magdeburg, (1990), see also http://www.femcos.de.
4. Gabbert, U., Altenbach, J.: COSAR - A reliable system for research and application (in German), Technische Mechanik, 11, (1990), Heft 3, 125-137.
5. Gotteland, M.: On theory for anisotropic and laminated plates, 3rd Int. Conf. on Structural Mechanics in Reactor Technology, Vol.5, Part M, Amsterdam, Oxford, North Holland Publishing Company, M5/4, (1975), 7.
6. Grigoliuk E. I., Chulkov P.P.: Nonlinear equations of thin elastic laminated anisotropic shallow shells with rigid filling, Izv. Akad. Nauk SSSR. Mekhanika, No. 5, (1965), 68-80.
7. Grigoliuk E.I., Kulikov G.M.: Multilayer reinforced shells: Calculation of pneumatic tires, Mashinostroenie, Moscow, (1988), 288.
8. Hsu T.-M., Wang J.T.-S.: A theory of laminated cylindrical shells consisting of layers of orthotropic laminae, AIAA Journal, Vol. 8, No. 12, (1970), 2141-2146.
9. Irons, B. M.: The Semiloof Shell Element. in Ashwell, D. G., Gallagher, R. H.: Finite Elements for Thin Shells and Curved Members. chapter 11, pp. 197-222, Wiley, (1976)
10. Mikhasev, G.I., Tovstik, P.E.: Stability of conical shells acted upon by external pressure, Izvestia AN SSSR, Mekhanika Tverdogo Tela, Vol.25, (1990), 99-104.
11. Tovstik, P.E.: Some problems of the stability of cylindrical and conical shells, Prikladnaya Matematika i Mekhanika, Vol. 47, (1983), 815-822.
12. Tovstik, P.E.: Stability of Thin Shells, Nauka, Moscow, (1995), 320.
13. Zienkiewicz, O. C.: The Finite Element Method. McGraw Hill Book Company Limited, (1977)

Addresses: Prof. Dr. Gennadi Mikhasev, Vitebsk State University, 33 Moskovsky Ave., Belarus — 210038 Vitebsk, e-mail: mikhasev@vgpi.belpak.vitebsk.by; Prof. Dr.-Ing.habil. Ulrich Gabbert, Dipl.-Ing. Falko Seeger, Institut für Mechanik, Otto-von-Guericke-Universität Magdeburg, Universitätsplatz 2, D-39106 Magdeburg, e-mail: ulrich.gabbert@mb.uni-magdeburg.de; falko.seeger@student.uni-magdeburg.de